Universidad de Valladolid

Escuela de Doctorado

# Trabajo Fin de Máster

Máster en Física

# Effect of carbon nanotubes on the thermal conductivity of flexible cellular polymers based on polyurethane

***Autor:***

*Antonio Cazurro Burgos*

***Tutor/es:***

*Ester Laguna Gutierrez*

*Miguel Angel Rodríguez Pérez*

# Abstract.

*The main aim of this research is to increase the thermal conductivity of flexible PU foams by the addition of single wall carbon nanotubes (SWCNT). Four techniques to maximise dispersion of nanotube in different mediums before its addition to a flexible Polyurethane (PU) matrix have been used. Semiempirical obtained solid conductivity values for all studied samples have been compared with theoretical models (mixing rule and Kapitza models), to assess whether filler percolation did take place or not. The effect of dispersion technique and percolation network in cellular structural changes has also been analysed. Net obtained thermal conductivity gain, directly attributed to addition of SWCNT is 25,6 %, referred to a pure flexible foam.*



**Key words:** PU foams, thermal conductivity, SWCNT, percolation network, dispersion technique, cellular structure.


# 1.-Introduction

Development of new polymeric materials with tailor made characteristics adapted to a wide range of functionalities have been made possible because of the huge development of polymer research since de 20th century until now. Among its most relevant features, good processability, light weight, low water absorption, high voltage breakdown strength and the most important, low cost, make them excellent candidates to be the starting point for striking new applications. In the last decades, composites, manufactured by addition of different fillersand nanofillers inside a polymeric matrix are becoming especially relevant. Among all of them, carbon nanotubes, discovered by Ijima in the 90´s, are one of the most interesting possibilities because of its outstanding mechanical, thermal and electrical characteristics.

Inside the segment of thermal applications, single wall carbon nanotubes (SWCNT´s) and Multiwall carbon nanotubes (MWCNT´s) present high conductivity values (range is within 3000-6000 W/mK) which has been evaluated both theoretically [1] and experimentally [2] [3] [4].

Due to these very high values of the thermal conductivity, many attempts have been made to increase the thermal conductivity of a polymer matrix by the addition of SWCNT/ MWCNT. Some of the most relevant papers are summarised in table 0.

**Table 1** Summary of some previous relevant reports where carbon nanotubes have been added to increase the thermal conductivity of a polymer matrix.

| Composite | Filler load | Δλ (W/ m K) | Production method | source |
|---|---|---|---|---|
| PVDF - SWCNT | Volume fraction > 49% | 130% | Hot processing | [5] |
| PDMS -MWCNT | 0,1 – 2,0 phr | 10% | Roll Milling/ compression | [6] |
| PMMA-SWCNT | 1 – 4 wt% | 1000 – 1500% | Compression 1200 psi | [7] |
| Ethylene Vinyl Acetate - | 20 -30 wt% | < 1000% | Melt mixing/ extrusion | [8] |
| PP – SWCNT | 10 -15 wt% | 240% | Extrusion | [9] |
| PU-SWCNT | 0,5 – 2,0 wt% | 42% | Polyol – CNt dispersion | [10] |

Despite of promising results showed in table 1, little has been discussed regarding relationship between composite obtention process, percolation, orientation of the fillers (topologically oriented to maximise physical characteristic along a specific axis) and the thermal conductivity so that is really difficult to assess whether the increase of the reported values maintain the overall performance of the remaining physical properties at the same performance level or there are some collateral effects. On the other hand, little attempts have been made in the spectra of polymer foams with open cell structure: sources from table 1 are referred mainly to solid materials (not foams).

Flexible cellular materials are widely used in industry as cushioning materials. Among them, free-rising polyurethane foams are one of the best known, as they can be obtained easily at a low cost. Two main reactions take phase during manufacturing process; while polyol and isocyanate reaction creates urethane bonds, there is also generation of $CO_2$ ,because chemical interaction of water and isocyanate. Both reactions take place simultaneously in a competitive way and are equally suitable, balanced by addition of catalysts and surfactants. Therefore, final material is composed by a solid phase, where polymer is structured in a network built up by indexes, struts and walls. Gas phase is sometimes retained inside within solid phase (closed cell foams) and sometimes not (open cell foams, interconnectivity in cellular structure is observed) depending which kind of final physical properties are sought. Addition of carbon fillers in flexible PU foams is seldom observed in literature [11] . An innovative application of this flexible material is presented here, joining cushion properties of flexible foam with the high potential that SWCNT have for enhancing thermal conduction: "cool effect"

term is normally linked with applications where flexibility, heat dissipation or heat transmission must be joined together (bed mattresses, travel space suits,…).

One of the main drawbacks that must be tackled before profiting on SWCNT properties in the field of composite materials is the big difficulty of getting an efficient dispersion in a non polar matrix, as fillers are heavily entangled and joined by Van der Waals bondings [12]. Dispersion technique plays an important role on this issue and must to be adapted to polymer matrix. [13].

The main aim of this research is the increase of the thermal conductivity in flexible polyurethane (PU) foams by addition of SWCNT. Several dispersion techniques have been employed [14] [15] and some of them have been implemented to ensure the highest nanotube dispersion before the production of the foam. To assess whether filler percolation did arrive to threshold, thermal conductivity of manufactured produced batches was tracked and results were confronted with full percolation model (mixing rule model) and intermediate model [16], focused on the concept of interfacial resistance developed by Kapitza. Using this approach, it has been possible to establish the improvements on thermal conductivity and to establish the best approach to disperse the fillers in the polymeric matrix.

# THEORETICAL BACKGROUND.

For one dimensional steady state heat flow, heat conduction rate can be expressed according to Fourier´s equation

$$q = -G\,\lambda A\frac{dT}{dx} \qquad (0)$$

Where λ is the thermal conductivity (W/ m K); A is the sectional area in ($m^2$) , $\frac{dT}{dx}$ is the temperature gradient across hot and cold sources and "G" is a correction factor for a given apparatus (see section 2.3 of characterisation techniques for details).

Heat transfer though a foam takes place by the contribution of four different mechanisms: 1) conductivity through polymer matrix; 2) conductivity through gas phase; 3) convection term; 4) radiative term. It is then stated that total foam thermal conductivity could be expressed as

$$\lambda = \lambda s + \lambda g + \lambda conv + \lambda r \qquad (1)$$

This concept is an accurate approximation except for cases in which low-emissivity boundary layers are used. In that case the actual effect on the foam conductivity will be far less than predicted by assuming that radiation acts independently of the other heat transfer mechanisms. [17] [18]

The different contributions of the previous equation can be modelled using the following equations:

1) conductivity of solid polymer phase can be expressed [17]

$$\lambda s = \frac{1}{3}\,Vs\,fs\,\lambda solid\,\sqrt{R} + \frac{2}{3}\,Vs\,(1-fs)\lambda solid\,\sqrt[4]{R} \qquad (2)$$

$$Vs = \frac{\rho f}{\rho s} \qquad (2.1)$$

Foam density and solid PU density are $\rho_f$ and $\rho_s$ respectively, and Vs corresponds to volume fraction of solid; R is the cell anisotropy ratio (ratio between cell size in the heat conduction direction and the cell size in the perpendicular direction to the heat flow) and $f_s$ the fraction of mass in the struts (i.e. ratio of the amount of solid phase in the struts of the cellular structure (edges and vertex) over the totality of solid phase (edges, vertex and walls). Unless specified, a value of 0,7 for $f_s$ will be used in this research which is a typical value for PU foams [19]. Value considered for pure PU solid ($\lambda solid$) is 0,26 W/mK [20]

2) conductivity of gas phase

$$\lambda g = Vg\,\lambda gas \qquad (3)$$

$V_g$ corresponds to volume fraction of gas phase within foam; a value of 0,0255 $Wm^{-1}K^{-1}$ has been used (conductivity of air at 25ºC and atmospheric pressure) [21].

3) Contribution of convection has been experimentally neglected due to the small cell size of the foams [18]. It is widely accepted in the literature [22] that this mechanism does not play a significant role if the cell sizes are smaller than 2 mm in diameter.
4) Radiative term contribution has been estimated by using Rosseland model [17] :

$$\lambda r = \frac{16n^2\sigma T^3}{3\text{Ķ}G} (4)$$

Where T is the Temperature. It is assumed that refractive index n is near 1 for polymer foams with low densities [17]. The value considered for Stefan Boltzmann constant (σ) is 5,6704 E-08 W/ $m^2 K^4$ [21].

Glicksman extinction coefficient $\text{Ķ}_G$, which is a theoretical value, can be estimated using equation 5. It represents radiation mean free path within the polymer foam before its total absorption, and it is usually expressed in $cm^{-1}$ or $m^{-1}$. Regarding this model, extinction coefficient is a function of densities of solid and foam, fraction of mass in struts (fs), cell size ($\phi$) and $\text{Ķ}_w$, which is the extinction coefficient for pure solid PU. Value considered for $\text{Ķ}_w$ is 60.000 $m^{-1}$ as per [17].

$$\text{Ķ}G = 4{,}10 \frac{\sqrt{fs\frac{\rho f}{\rho s}}}{\phi} + (1 - fs)\frac{\rho f}{\rho s}\,\text{Ķ}w \quad (5)$$

The strategy that was set to assess the contribution of carbon nanotubes in overall foam thermal conductivity on each studied sample is summarized as follows.

a.-Remove from total measured values of thermal conductivity gas phase and radiative terms (ec.1). Output value is foam $\lambda s$.

b.- Calculation of $\lambda_{solid}$ (conductivity of bulk polymeric material) for obtained composites by using ec.(2). Real values of $\rho_s$ (1242 kg/ $m^3$ considered for solid PU according supplier technical datasheets, in phase with other publications [23] ) and . $\rho_f$ (foam density measured, (see section 3 for details) are considered. Cell size $\phi$ and anisotropy ratio were also experimental values measured (section 3, table 4 for details). Expected obtained value must to be equal (no percolation) or higher (percolated SWCNT´s) than 0,26 W/mK set for pure solid PU.

c.- Estimate a normalized foam conductivity going back to ec. 2) and 1) but considering for all samples a standard foam density value ($\rho_f$ ) of 56,3 kg/$m^3$ ,obtained from a reference sample with no carbon nanotubes (see tables 2 and 3). Normalized values are also referred to same $f_s$ and anisotropy ratio (R), 0,7 and 1 respectively. In figure 1 there is a summary to explain these steps for better understanding.

**Fig.1** Summary of procedure followed for obtention of normalised thermal conductivity of a foam.

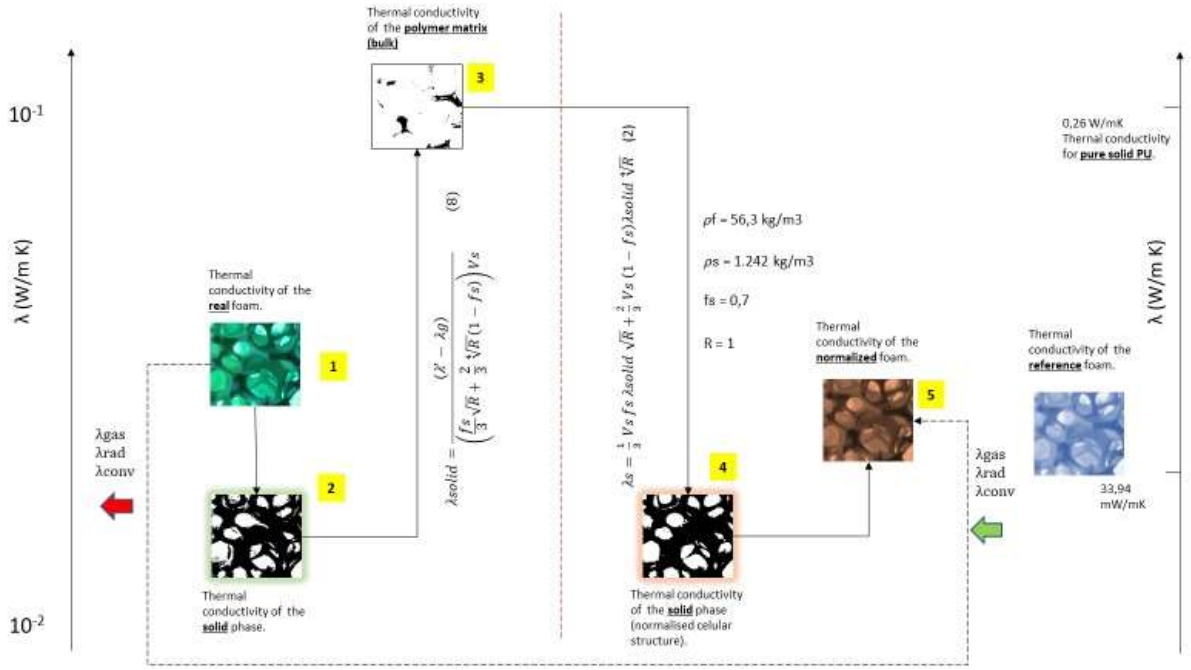

# 2.-Experimental

## 2.1 Materials.

*A Premixture* of several raw materials is obtained by the addition of 86,9 wt% of a commercial polyol A (48mg KOH/g; visc. 560 CP a 25ºC; PM 3.500 gr/ mol), 7wt% distilled $H_2O$ 1,0 wt% catalyst A, 4,9 wt% surfactant A, 0,2 wt% catalyst B. All described components are poured inside a plastic cup and mechanically stirred (shear mixing) at 250 rpm during 3 min. The premixture stays under optimum conditions no longer than 48h since manufacturing date. After that period a brand-new premixture batch must to be produced.

*A toluene derivative commercial isocyanate (TDI) was used in all produced samples* with a purity 99,5 wt%, density 1,22 gr/cm$^3$, Molecular weight, W, 174,15 gr/mol.

*Single Wall Carbon Nanotubes (SWCNT):* Two kind of commercial products have been used, both of which have been kindly supplied by OcSiAl™. *1) Tuball SWCNT™*, purity 74,0 +/- 1,5 % (from now on, considered as "cnt1" filler type). *2) Dispersion Tuball Matrix 202™* that contains carbon nanotubes previously predispersed by supplier at 10 wt % in a glycydil ester of density 0,95 gr/cm$^3$ (from now on, considered as "cnt2" filler type). Density considered for carbon nanotubes is 1,7 gr/ cm$^{3.}$ For a single carbon nanotube, average diameter is 1,50 nm; average length is 1,7 μm according technical datasheet. Unless specified, concentration of pure carbon nanotubes (CNT) referred in next sections is going to be referred to 100 parts of total polyol added in the formulation (parts per hundred parts of polyol, pph).

*Pure PU foam production*: Pure or reference batches have been performed by the addition of 58,18 wt% commercial polyol B (32mg KOH/g; visc. 1350 CP a 25ºC; PM 5.000 gr/ mol.) and 22,32 wt% of premixture. Components are stirred at 2.000 rpm during 5 minutes. Isocyanate (19,50 wt%) is then poured in reactor and resultant mixture is again stirred at 2.000 rpm during 10 seconds. Resultant foam must be kept stored at least 48h at 25ºC before characterisation.

*Masterbach.* Different masterbatches have been used, depending on the process strategy that is going to be followed (see table 2)

*Standard masterbatch (SM*), is produced by the addition of polyol B and 0,5 pph of pure CNT. Mixture is mechanically stirred as showed in table 2. As two kind of SWCNT are available, SM1 and SM2 are obtained from "cnt1" and "cnt2" filler types respectively.

Isocyanate masterbatch A is prepared by addition of 120 ml. of isocyanate (99,60 wt%) and carbon nanotubes (0,40 wt%). Mixture is poured in an erlenmeyer cooled in a water bath at 25ºC and it is probe sonicated (Vibracell sonic processor 750 W, 20KHz, Amplitude 40%) by directly applying over dispersion a set of pulses of 3 seconds. An interval time of 2 seconds is left between each sonication. Pulses are repeated until overall time of 40 minutes is reached. All the process must to be done in a vacuum bell. As in the previous section, A1 and A2 are referred to the same dispersion procedure and SWCNT concentration but different specifications ("cnt1" and "cnt2" respectively).

*Isocyanate masterbatch B*. is prepared by the addition of 120 ml. of isocyanate (99,02 wt%) and pure carbon nanotubes (0,98 wt%). Mixture is poured in an Erlenmeyer and follows same procedure as masterbatch A. Masterbatches B1 and B2 are referred to the same dispersion procedure and CNT concentration but different specification of CNT.

Four strategies have been set to maximise dispersion of carbon nanotubes within masterbatches, a summary is detailed in table 2. In is important to said that in strategy 1, "SM1" and "SM2" masterbatches are directly obtained by mixture of polyol "B" and carbon nanotubes and mixture is shear-mixed at 2000 rpm during 5 minutes. In strategy 2, there is a previous sonication of CNT´s in a dispersive medium (same sonication parameters as per masterbatches "A" and "B") before first dispersion was poured in polyol "B. Afterwards mixture is mechanically stirred during 5 min (IKA T25 Digital disperser Ultraturrax™ 3000 rpm). and left in a vacuum boiling conditions to remove solvent. Dispersive mediums that have been tried for strategy nr.2 are acetone (Scharlau, purity 99,5%, density 0,787 g/cm3 (20ºC)), and isopentane (Scharlau, purity 95%, density 0,625 g/cm3 (20ºC)). Strategy 4 is nearly similar to strategy 3, with the only difference of two sonications instead of one.

*Flexible foam composites.* Formulas that have been followed for production of foam composites with SWCNT are similar from that of pure/ reference foams, already described at the beginning of this section, but adapted to SWCNT addition.

In table 3 a summary of main components used and proportions (wt%) per process strategy is detailed. All strategies follow the similar overall mixing rates (wt%) for all components, but procedures followed for enhancing dispersion of carbon nanotubes are significantly different.

**Table 2.** *Summary of the main strategies followed by obtention of CNT masterbatch.*

| | | First dispersion | Second dispersion | Masterbach |
|---|---|---|---|---|
| | 1.- CNT mixture + dispersive medium. | 2.- US stirring 40 min. 3/2 pulses **(Predispersive medium)** | 3.- first dispersion+ poliol B.<br>4.- Mechanical stirring with Ultraturrax 5 min. | 5.- Masterbach manufacturing |
| Nº1 Shear (mechanical mixing) | SWCNT + polyol B | No | No | Shear mixing 2000 rpm 5 min.<br>SM1 and SM2 are obtained. |
| Nº2 PUS + ULTX | SWCNT in:<br>1) Acetone.<br>2.- Isopentane. | Yes, x1 sonication; 40 min; 3/2 pulses | Yes | Vaccum boiling of dispersant medium + magnetic stirring 3h.<br>SM1 and SM2 are obtained. |
| Nº3 iscn ("on site") | SWCNT + commercial isocyanate | Yes, x1 sonication; 40 min; 3/2 pulses | No | Dispersion A1; A2 (flexible foam 0,1 pph CNT)<br>Dispersion B1; B2 (flexible foam 0,25 pph CNT) |
| Nº4 iscn ("on site") | SWCNT + commercial isocyanate | Yes, x2 sonications; 40 min; 3/2 pulses | No | Dispersion A1; A2 (flexible foam 0,1 pph CNT)<br>Dispersion B1; B2 (flexible foam 0,25 pph CNT) |

It is important to remark that addition of carbon nanotubes is never made directly, but always through a masterbatch that could have polyol B or isocyanate as a dispersive medium. SM1 masterbach (filler source is a "cnt1" non predispersed SWCNT) is used for obtention of 0,1 and 0,25 pph foam composites by changing weight proportion; SM2 masterbatch is also used to obtain 0,1 and 0,25 pph of foam composites from a predispersed SWCNT filler source. Isocyanate masterbatch "A" is mainly used to obtain composites of 0,1 pph and isocyanate masterbatch B is mainly used to obtain composites of 0,25 pph.

Mixing sequence is also detailed in table 3 in brackets. In strategies 1 and 2 polyol B, masterbatch SM and premixture are stirred at 2.000 rpm during 5 min. Then, pure isocyanate is added and final mixture is stirred again at 2.000 rpm during 10 seconds. In strategy 3-4 polyol and premixing are stirred at 250 rpm during 3 min, then mixture is collected in the same syringe and added in reactor. Afterwards isocyanate masterbatch A or B are also injected inside reactor and final mixture is stirred at 2.000 rpm during 10 seconds.

**Table 3** Summary of formulations employed per process strategy. Data are indicated in wt%. Number in brackets correspond to mixing step.

| | | | Standard Masterbatch | | | | | Isocyanate Masterbatch | | | |
|---|---|---|---|---|---|---|---|---|---|---|---|
| **Strategy** | **Filler Itype** | **Filler load (pph)** | **Polyol B (wt%)** | **SM1 (wt%)** | **SM2 (wt%)** | **Premixture (wt%)** | **Pure isocyanate (wt%)** | **A1 (wt%)** | **A2 (wt%)** | **B1 (wt%)** | **B2 (wt%)** |
| Pure | none | None | 58,18 (1) | --- | --- | 22,32 (1) | 19,50 (2) | --- | --- | --- | --- |
| Strategy 1-2 | cnt1 | 0,1 | 42,63 (1) | 15,58 (1) | --- | 22,30 (1) | 19,49 (2) | --- | --- | --- | --- |
| Strategy 1-2 | cnt2 | 0,1 | 42,34 (1) | --- | 16,16 (1) | 22,15 (1) | 19,35 (2) | --- | --- | --- | --- |
| Strategy 1-2 | cnt1 | 0,25 | 19,36 (1) | 38,91 (1) | --- | 22,28(1) | 19,45 (2) | --- | --- | --- | --- |
| Strategy 1-2 | cnt2 | 0,25 | 19,02 (1) | --- | 39,95 (1) | 21,89 (1) | 19,14 (2) | --- | --- | --- | --- |
| Strategy 3 - 4 | cnt1 | 0,1 | 58,13 (1) | ---- | --- | 22,30 (1) | --- | 19,57 (2) | --- | --- | --- |
| Strategy 3 - 4 | cnt2 | 0,1 | 57,73 (1) | --- | --- | 22,15 (1) | --- | --- | 20,12 (2) | --- | --- |
| Strategy 3 - 4 | cnt1 | 0,25 | 58,07 (1) | --- | --- | 22,28 (1) | --- | --- | --- | 19,65 (2) | --- |
| Strategy 3 - 4 | cnt2 | 0,25 | 57,07 (1) | --- | --- | 21,89 (1) | --- | --- | --- | --- | 21,04 (2) |

## 2.3 Characterisation techniques.

*Thermal conductivity.*

Thermal conductivity was measured by the Transient Plane Source (TPS) technique using a thermal conductivimeter mod. HDMD (Hotdisk). The basic principle of this method relies in a plane element that acts both as temperature sensor and heat source. Source is constructed from a two-sided nickel foil resistance (10 μm) inserted amidst two insulant foils made from kampton (70 μm). The resistance radius is 3,189 mm, the average power source is 0,006 W, the measuring time is 40 seconds. Measures have been made four times; a time split of 5 minutes between consecutive measurements is left to avoid temperature drift.

The TPS element is placed between two samples of standard size 30 x 30 x 30 mm. It is important to specify that in all measured samples have been oriented in the way that foam growing direction is parallel to the heat flow. This method is quick, versatile and allows us to compare conductivity of the different materials produced. However, discrepancies between values obtained by this method and steady state conditions have been reported [24]. TPS measurements provides higher conductivity values than steady state heat flow conditions. Despite of its accurateness, equipments that work under steady-state conditions require samples with a higher size, and also higher operation times that makes them unsuitable for this research. To solve this issue, a well-known characterised reference sample, which conductivity has been evaluated by steady state flow method was taken as a background that was confronted with measure taken on the same sample by TPS method. Consequently, a correction factor (G) of 0,62 has been set in equation (0). It is important to emphasize that trends observed in steady -state methods because variations on density, cellular structure, and filler addition are equally observed by TPS method at a similar level of sensitivity and within the same measurement ranges [24].

*Density.*

As studied PU foams in this work are open cell materials, density characterization has been obtained through geometric method. Size of the samples was measured with a digital caliper with precision 0,01 mm, weight was measured with precision of 0,0001 g. Three measurements of each characteristic have been performed per sample, then an average value of overall density was obtained.

*Cellular structure characterisation by scanning electron microscopy (SEM).*

*Preconditioning of samples; metallization*. A 5 nm thick gold layer is deposited over the samples by means of a SCD 004 Balzers equipment. Samples are previously stuck on a metallic holder by mean of a carbon double side adhesive tape. Then, holder is placed inside the chamber. Argon acts as a removal gas to avoid trapped free particles over samples during metallisation process. Then a vacuum of 0,05 mbar is applied, and a source of 30 mA is maintained during 40 sg. Therefore, gold is vaporised and goes through sample.

*Cellular characterisation* has been made with a Hitachi FlexSEM 1000 with filament made from Wolframium. Sputtered electrons over sample are generated by thermo ionic effect. The accelerating voltage was 10 keV, working distance (WD) 38,3 mm, emission current 0,112 mA. All the obtained SEM images have been taken using the same scale for better comparison among them. Measure of relevant key parameters of cellular structure were obtained with specialized software based on Image J/ Fiji[25]. This software provides the cell size distribution, average cell size, standard deviation of the cell size and anisotropy ratios. Relevant measurements of cell structure for all produced flexible PU - SWCNT composites are summarised in table nr.4

# 3.- Results and discussion.

## 3.1.- Characterisation of cellular structure.

A summary of the main measured cell parameters is showed in table 4. Each sample is identified with a number that will be used in the rest of the manuscript. Cell sizes values ranges from 635 to 1077 μm and anisotropy ratios (R) from 1,0 to 1,6. Anisotropy ratio is defined as the relationship between cell size in y-axis (foam growing direction) vs. x-axis. Density and measured thermal conductivity are also included as other relevant physical properties. Range for measured thermal conductivity of samples goes from 33,94 (reference sample) to 47,82 mW/mK,. It is relevant to say that there are two samples (nr.16 and 17) which have outstanding conductivity values. These values are only approached by another two samples (numbers 2 and 12)

Six samples have been considered as the most representative, and its cellular structure has been analysed. using SEM pictures (figs. 2 to 5) **Pure sample nr. 4** (33,94 mW/ m K) is chosen as a background reference to be compared with samples containing carbon nanotubes: **sample nr. 3** was chosen because this is the sample with the lowest anisotropy ratio (1,0), cell size near the highest interval value (mean value is 829 μm) and thermal conductivity near the lowest values (34,27 mW/ m K).**Sample nr. 13** has a "R" between the two limiting values (1,3) and a conductivity in the medium- low

position inside the interval (36,51 mw/m K). **Sample nr. 6** has been chosen because it has the highest cell size (1077 μm) and one of the highest "R" (1,5). In the case of **sample nr. 11**, obtained value for λ is near the middle position of the interval (37,97 mw/ m K); cell sizes (964 μm) and anisotropy ratios (1,4) are among the highest values. Finally, samples 15 and 16 have been chosen as they have the highest thermal conductivities, measured values (47,82 and 43,15 mW/ m K respectively).

***Table 4.*** *Results of foam samples characterisation, where cnt1 are standard SWCNT and cnt2 predispersed SWCNT.*

| Nr. | Process strategy | Dispersive medium | Filler type | Filler load (pph) | Foam density (kg/m³) | Cell size (μm) | Cell size_standard deviation. | Anisotropy ratio (R) | Thermal conductivity $\lambda_m$ (mW/m K) |
|---|---|---|---|---|---|---|---|---|---|
| **1** | strategy 1 | Polyol | cnt1 | 0,10 | 82,2 | 635 | 225 | 1,0 | 34,20 |
| **2** | strategy 1 | Polyol | cnt1 | 0,25 | 104,3 | 828 | 321 | 1,5 | 39,66 |
| **3** | strategy 1 | Polyol | cnt2 | 0,10 | 191,9 | 829 | 434 | 1,0 | 34,27 |
| **4** | strategy 1 | Polyol | reference | 0,00 | 56,3 | 600 | — | 1,0 | 33,94 |
| **5** | strategy 2 | Acetone | cnt2 | 0,10 | 77,9 | 705 | 208 | 1,5 | 36,75 |
| **6** | strategy 2 | Isopentane | cnt2 | 0,10 | 76,6 | 1077 | 463 | 1,5 | 36,86 |
| **7** | strategy 2 | Acetone | cnt2 | 0,01 | 78,4 | 635 | 244 | 1,4 | 34,06 |
| **8** | strategy 2 | Isopentane | cnt2 | 0,25 | 103,6 | 726 | 310 | 1,0 | 36,55 |
| **9** | strategy 2 | Acetone | cnt2 | 0,10 | 75,4 | 680 | 265 | 1,3 | 33,20 |
| **10** | strategy 3 | Isocyanate | cnt1 | 0,10 | 75,2 | 744 | 440 | 1,4 | 37,17 |
| **11** | strategy 3 | Isocyanate | cnt2 | 0,10 | 94,1 | 964 | 336 | 1,4 | 37,97 |
| **12** | strategy 3 | Isocyanate | cnt1 | 0,25 | 69,9 | 854 | 380 | 1,5 | 37,52 |
| **13** | strategy 3 | Isocyanate | cnt1 | 0,10 | 91,0 | 699 | 232 | 1,3 | 36,51 |
| **14** | strategy 3 | Isocyanate | cnt2 | 0,10 | 80,6 | 751 | 255 | 1,6 | 36,93 |
| **15** | strategy 4 | Isocyanate | cnt2 | 0,25 | 87,8 | 677 | 237 | 1,2 | 47,82 |
| **16** | strategy 4 | isocyanate | cnt1 | 0,10 | 74,5 | 744 | 271 | 1,4 | 43,15 |

SEM_ picture of reference sample is showed in fig.2. Regular cell size distribution is evident, preferential orientation is not observed in any specific axis. Fraction of mass is also observed in cell walls, but cell interconnectivity is clear.

***Fig.2*** *SEM picture obtained from sample nr.4 (pure reference).*

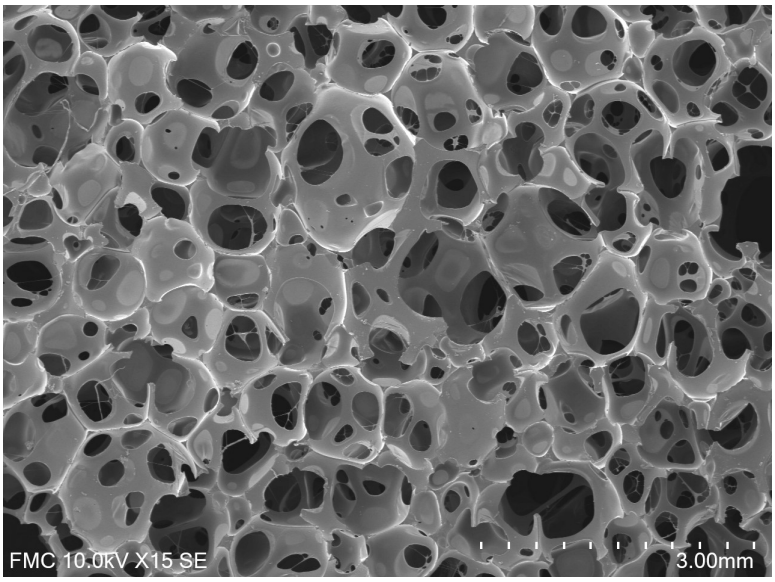


**sample nr. 4 (reference):** strategy 1. Cell size 600 μm ; density 68,7 kg/ m3; $\lambda_{foam}$ 33,94 mW/m K R= 1,0

**Sample nr.3** (fig.3) presents a non-regular cellular structure, which is distorted. It is not seen a clear cell orientation in any specific axis. The main differences with reference sample (Fig. 2) is that cell size distribution is displaced towards higher

values; it is also observed a higher fraction of mass in cell walls compared with the other selected samples, which is confirmed by higher density value of this sample (191,3 kg/m$^3$). **Sample nr.13** has a similar cell size distribution than reference sample, also fraction of mass in the cell walls is qualitatively observed to be similar to the reference, but higher density than reference was measured (91,0 kg/m$^3$ ).

***Fig.3***.

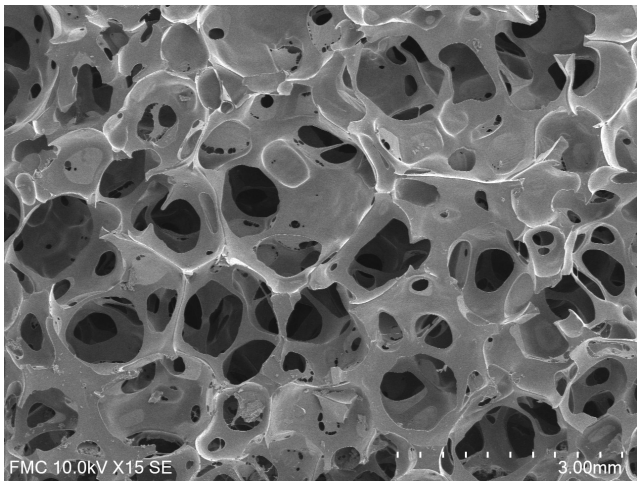


**sample nr. 3:** strategy 1. Cell size 829 μm; density 191,3 kg/ m3
$\lambda_{foam}$ 34,27 mW/m K R= 1,0

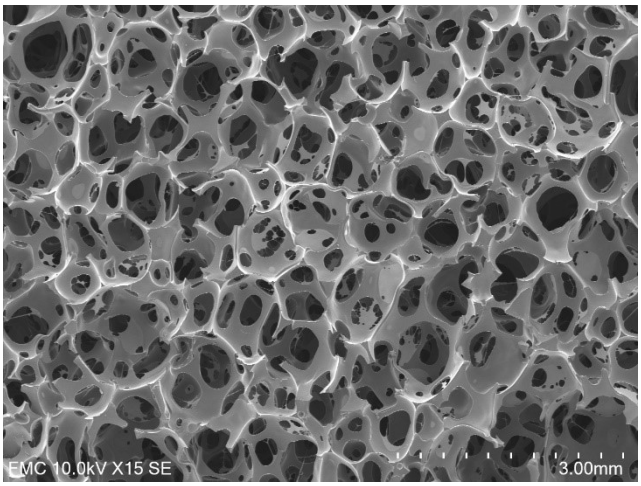


**sample nr.13:** strategy 3. Cell size 699 μm; density 91,0 kg/ m3;
$\lambda_{foam}$ 36,51 mW/m K R=1,3.

Sample nr. 6 showed in fig.4 present a clearly defined cell orientation in the growing direction. A closed cell structure is observed in some relevant areas of SEM picture, which can limit cell interconnectivities, still observed at a minor rate. However, in sample nr. 11 interconnectivities are clearly perceived, fraction of mass in struts is more relevant and some particular areas present cells with broken struts.

***Fig.4***

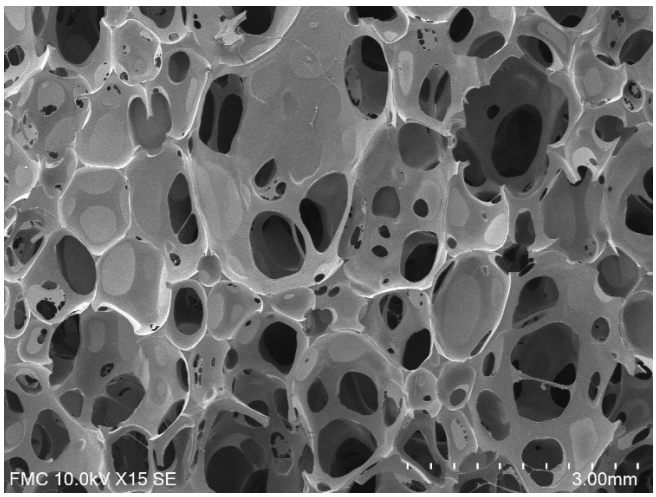


**sample nr. 6:** strategy 2 Cell size 1077 μm; density 76,6 kg/ m3;
$\lambda_{foam}$ 36,86 mW/m K R= 1,5.

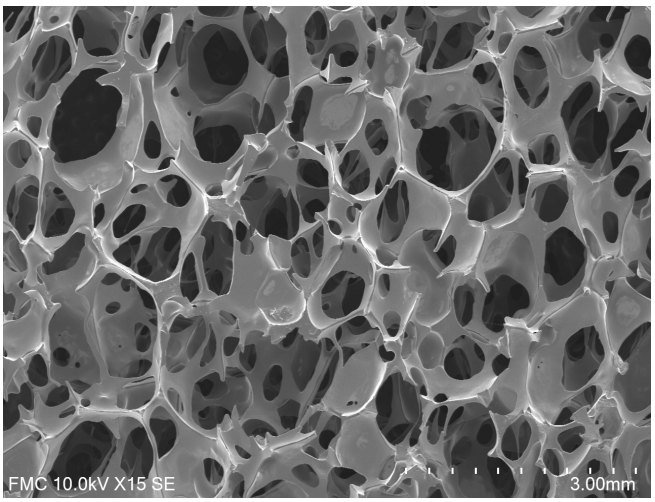


**sample nr. 11:** strategy 3 Cell size 964 μm; density 94,1 kg/ m3;
$\lambda_{foam}$ 37,97 mW/m K R= 1,4.

Finally, in fig.5 it is presented a set of micrographies which belong to the two samples with the highest obtained conductivity values.

Change of morphology on cellular structure that begun to be observed in sample nr. 11, becomes here more important. Structure is so dramatically changed that has been hardly difficult to obtain a set of values which could be considered as sample representative. There are big voids where cell measurements have not been possible to perform, because of broken struts. It is important to emphasize that despite observed variations, interconnectivities between adjacent areas still are observed.

**Fig. 5**

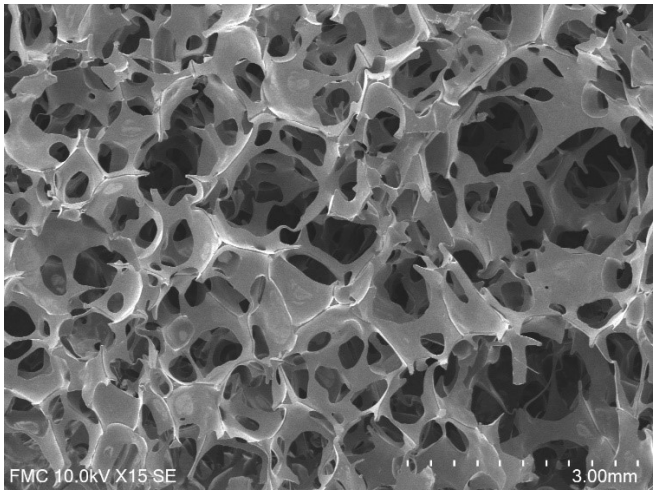


**sample nr. 16:** strategy 4_Cell size 744; density 74,5 kg/ m3; $\lambda_{foam}$ 43,15 mW/m K R= 1,4.

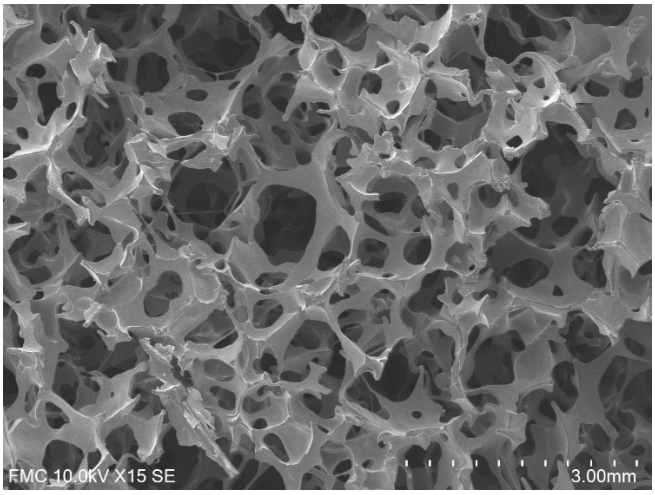


**sample nr. 15:** strategy 4_Cell size 677; density 87,8 kg/ m3; $\lambda_{foam}$ 47,82 mW/m K R= 1,2.

## 3.2.- Effect of process strategy on density and anisotropy ratio.

*Density.*

The addition of SWCNT increases the viscosity of solid phase before polymerization, which might the affect foaming process and thus final foam density. In fact, the foams containing carbon nanotubes have higher densities than the reference foam (see table 4). Election of the most suitable technique must ensure optimum SWCNT dispersion inside the matrix by adjusting final density to its optimum level. In fig.6 it is explained the effect of process strategy on final average density obtained value (left). It is also showed the effect of SWCNT type of filler source on final obtained density (right). Strategy 1 provides the highest and most randomly distributed density values. No relevant differences are detected among the remaining three strategies (average is approximately 80 kgr/ $m^3$). This result can be explained by the fact that shear mixing used in strategy 1 is not enough to disperse SWCNT in a high viscosity medium. Contribution of predispersed SWCNT to the final density is also higher (right), as it is needed to add more commercial product to obtain the same filler pph load (1 part of filler per 9 parts of dispersive medium as per section 2.1).

Anisotropy ratio (R).

Anisotropy ratio plays a relevant role in overall foam heat flow mechanism. A cellular structure oriented in y-axis (R>1) is suitable to obtain a higher thermal conductivity in that directions [17]. Fig. 7 (left) summarises contribution of process strategy to average anisotropy obtained ratios. Strategy 1 presents the lowest anisotropy ratios because cellular structure is often distorted as was seen in previous section. Strategy 3 presents the highest anisotropy values. There is a clear discrepancy between strategy 3 and 4 obtained values, which is especially interesting as both strategies are quite similar, but obtained values from strategy 4 are even less than obtained from strategy nr.2. These discrepancies are attributed to the modification of the cellular structure, already explained in previous section. Fig. 7 (right) summarises contribution of source of filler load to "R". Filler type does not have a clear influence on the final anisotropy ratio, which is mainly linked to process strategy.

**Fig.6** *Contribution of process strategy to average density values obtained from manufactured samples (left). Contribution of SWCNT source is specified at right. Thick bars represent average density values. Thin lines at the top represent standard deviation.*

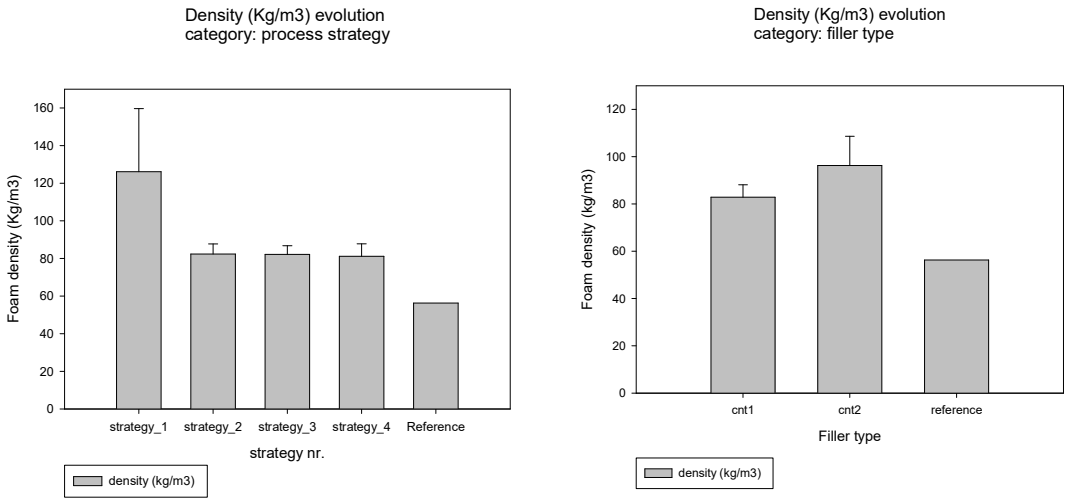


***Fig.7*** *Contribution of process strategy to average anisotropy ratios obtained from manufactured samples (left). Contribution of SWCNT source is specified on the right). Thick bars represent average density values. Thin lines at the top represent standard deviation.*

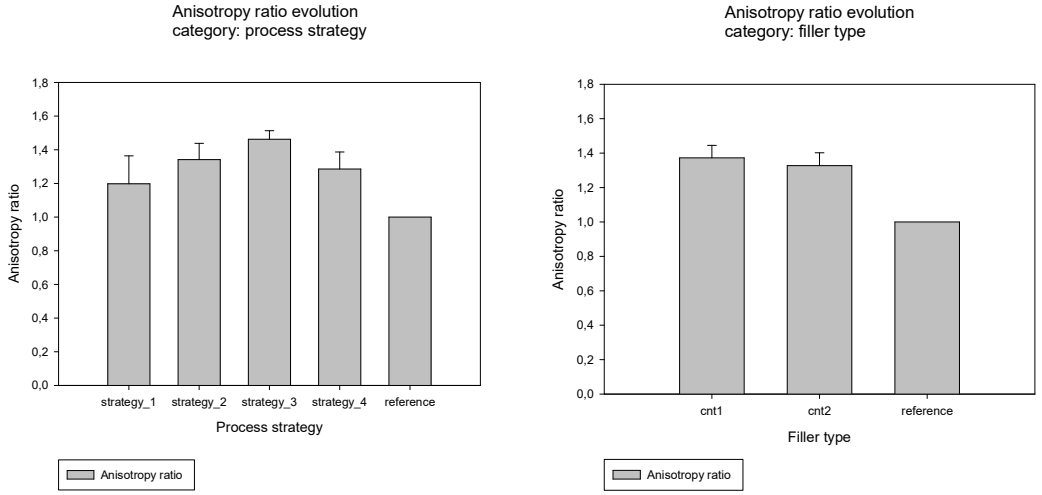


*Correction of overall thermal conductivity. Assessment of direct SWCNT´s contribution.*

As explained in theoretical background, (ec.2), high densities and anisotropy ratios also have a positive effect on the increase of overall foam´s thermal conductivity, therefore these contributions must be isolated from the overall conductivity obtained values, as the scope of this work is to assess the main contribution of -SWCNT´s apart from other indirect factors.

Conductivity of polymeric matrix $\lambda_{solid}$ could be obtained from equation (1) and (2):

$$\lambda` = \lambda - \lambda r - \lambda conv \qquad (6)$$

When λ' is obtained by subtracting radiative and convective terms from total measured conductivity value. Convection term is negligible as explained in previous sections. From equation (2)

$$\lambda` - \lambda g = \frac{1}{3} Vs\ fs\ \lambda solid \sqrt{R} + \frac{2}{3} Vs\ (1 - fs) \lambda solid\ \sqrt[4]{R} \qquad (7)$$

Then, conductivity of polymeric matrix, λsolid, could be expressed as

$$\lambda solid = \frac{(\lambda' - \lambda g)}{\left(\frac{fs}{3}\sqrt{R} + \frac{2}{3}\sqrt[4]{R}(1-fs)\right)Vs} \quad (8)$$

Anisotropy ratio R and Vs (volume fraction for solid) could be obtained from table 4. Obtained λsolid for all produced samples using equation (8) are summarised in table 5. Figure 8 summarizes λsolid obtained values for all samples, split by process strategy. A threshold value of 0,26 W/ m K (red dotted line) was considered for conductivity of pure PU solid ($\lambda_{PU\,s}$) (without SWCNT´s, ) [20] [26] The materials produced from strategies 3 and 4 systematically show value of λsolid higher than that of the reference, the highest value is that obtained from sample 15 obtained using dispersion strategy 4.

Normalised foam conductivity (i.e thermal conductivity for samples with the same density and anisotropy ratio than the reference sample, but with a different thermal conductivity of the solid phase) can be now obtained by introducing again λsolid values in ec (2), but now density value considered is that of the reference ( 56,3 kg/m$^3$ ) (density value for reference foam) instead of real value. Anisotropy ratio is considered 1,0 for all cases. Then, previously subtracted terms from (1) are added again ($\lambda_g$ and $\lambda_r$) to obtain normalised conductivity values (see fig.1), which are also specified in table 5.

Table nr.5 shows four conductivity values for λsolid (polymeric matrix) bellow threshold of 0,26 W/ m K (samples nrs. 1; 3; 7; 9, see fig.8). The explanation is that density correction was overrated. Equation (8) only considers a density augmentation due to a thickness increase of struts and walls within the cellular structure, which is not the case for these critical samples: the increase of density is due to bulk masterbach that was not built inside foam cell structure because of an inefficient stirring process. This effect is perceived specifically in strategies 1 and 2

***Table 5*** *Normalised thermal conductivity values per sample by correction of density and anisotropy effect.*

| Nr. | Process strategy | Dispersive medium | Filler type | Filler load (pph) | Volume fraction of solid $V_s$ | Conductivity of λsolid (W/m K) | Measured conductivity λ (mW/m K) | Normalised conductivity λ (mW/m K) |
|---|---|---|---|---|---|---|---|---|
| **1** | strategy 1 | Polyol | cnt1 | 0,10 | 0,0661 | 0,2297 | 34,20 | 32,55 |
| **2** | strategy 1 | Polyol | cnt1 | 0,25 | 0,0840 | 0,2965 | 39,66 | 33,76 |
| **3** | strategy 1 | Polyol | cnt2 | 0,10 | 0,1545 | 0,1529 | 34,27 | 29,82 |
| **4** | **strategy 1** | **Polyol** | **reference** | **0,00** | **0,0453** | **0,2600** | **33,94** | **33,94** |
| **5** | strategy 2 | Acetone | cnt2 | 0,10 | 0,0627 | 0,2782 | 36,75 | 33,82 |
| **6** | strategy 2 | isopentane | cnt2 | 0,10 | 0,0617 | 0,2601 | 36,86 | 34,22 |
| **7** | strategy 2 | Acetone | cnt2 | 0,01 | 0,0631 | 0,2036 | 34,06 | 32,14 |
| **8** | strategy 2 | isopentane | cnt2 | 0,25 | 0,0834 | 0,2708 | 36,55 | 33,08 |
| **9** | strategy 2 | Acetone | cnt2 | 0,10 | 0,0607 | 0,1824 | 33,20 | 31,92 |
| **10** | strategy 3 | isocyanate | cnt1 | 0,10 | 0,0605 | 0,2977 | 37,17 | 34,38 |
| **11** | strategy 3 | isocyanate | cnt2 | 0,10 | 0,0758 | 0,2763 | 37,97 | 33,79 |
| **12** | strategy 3 | isocyanate | cnt1 | 0,25 | 0,0563 | 0,3085 | 37,52 | 35,05 |
| **13** | strategy 3 | isocyanate | cnt1 | 0,10 | 0,0763 | 0,2623 | 36,51 | 33,13 |
| **14** | strategy 3 | isocyanate | cnt2 | 0,10 | 0,0649 | 0,2672 | 36,93 | 33,62 |
| **15** | strategy 4 | isocyanate | cnt2 | 0,25 | 0,0707 | 0,4477 | 47,82 | 42,62 |
| **16** | strategy 4 | isocyanate | cnt1 | 0,10 | 0,0600 | 0,2729 | 43,15 | 40,84 |

We can now go back to cellular structure of most representative samples and cross this information with position of samples vs. threshold value of 0,26 W/m K (fig.8): sample 3 (fig. 3) with distorted cellular structure, low anisotropy ratio and a high fraction of mass in cell walls is far below threshold value. Sample nr. 6 (fig. 4) with limited cell interconnectivity and a fraction on closed cells is in the limit. Sample nr. 13 with cellular structure which is similar to reference is also in the limit (fig. 3). Sample 11 (fig.4) with a high fraction of mass in struts and some damages in the cellular structure is over the limit, and finally samples 15 and 16 which exceeds by far threshold value presents a huge change of morphology in cellular structure, but interconnectivity is present (fig.5).

***Fig.8*** *Normalized* λsolid *(W/ mK) in all studied samples vs. threshold value of PU pure solid (0,26W/ mK; red dotted line). Data are split by process strategy.*

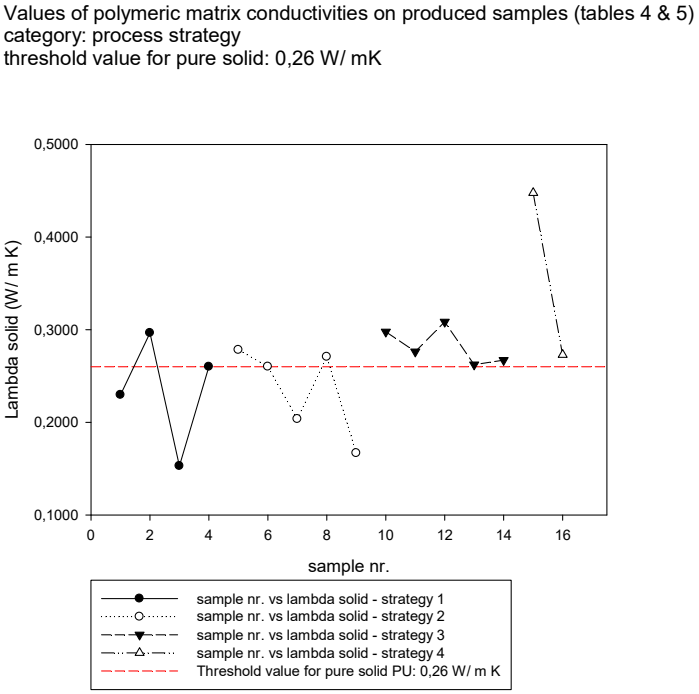


## 3.3 Analyse of normalised thermal conductivity obtained values.

In fig. 9 (left), average foam thermal conductivity values, obtained per process strategy are showed. It is interesting to highlight that despite strategy 3 provides better solid conductivity values than strategies 1 and 2 (fig.8), mean value is at the same level than reference. However, there is not any discrepancy with fig.8. The explanation is that radiative term in reference sample is more important than samples manufactured under strategy 3, which have a higher extinction coefficient because they have a higher volume fraction of solid $V_s$; gain by filler percolation has been cancelled by loss of radiative term. On fig.9 right, same values are split per type of filler load. The addition of predispersed carbon nanotubes has not any positive impact on the improvement of the thermal conductivity, even it is slightly negative. Regarding the effect of the filler load (fig.10), a loss of 1,0% is observed in average values vs. reference when filler load is 0,1 pph. This value must be compared with maximum gain achieved vs. reference in sample 16, also with 0,1 pph (40,84 mW/mK, gain of 20,3%). We can now conclude that by optimising dispersion technique we can get an improvement on thermal conductivity of a 20% approximately. We can do same calculation for 0,25 pph and we obtain a similar improvement rate: average gain vs. reference is 5,0%. This value is compared with improvement rate achieved by sample 15 (42,62 mW/mK) vs. reference, which is 25,6%. Therefore strategy 4 has the potential to be approximately a 20,4% more efficient when it is compared with the average values obtained from all strategies.

The main question that remains to be answered is whether this improvement achieved in process strategy nr. 4 has arrived to its maximum value or not. For that, we will confront real conductivity values with theoretical mixing rule and Kapitza models.

***Fig.9*** *Normalised foam thermal conductivity values br process strategy and filler type.*

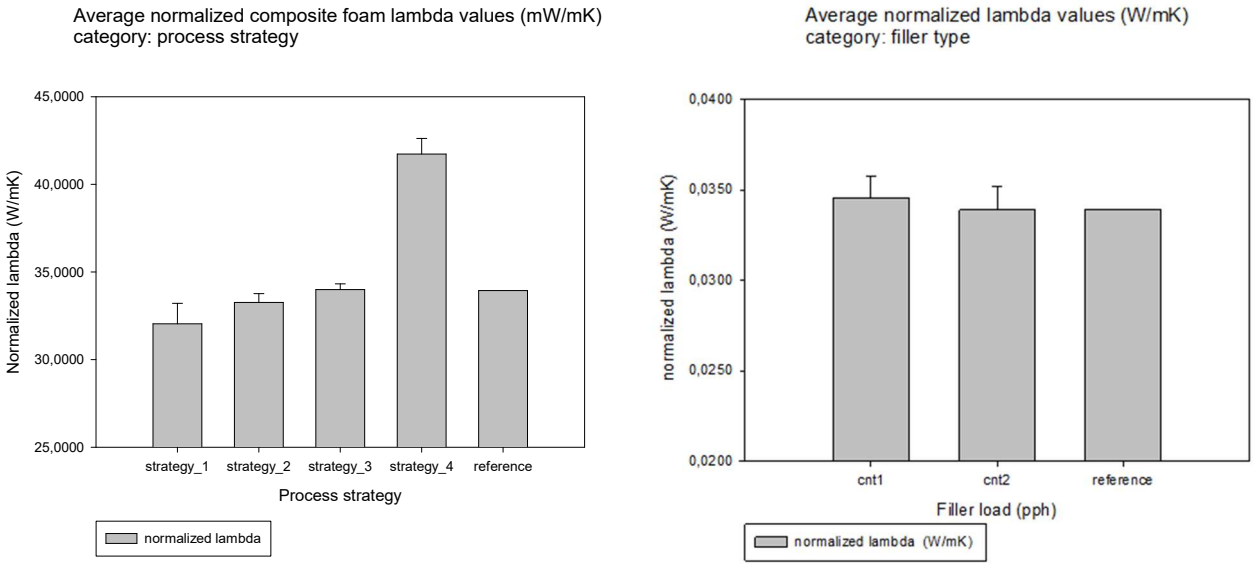


***Fig.10*** *Normalised foam thermal conductivity values by filler load.*

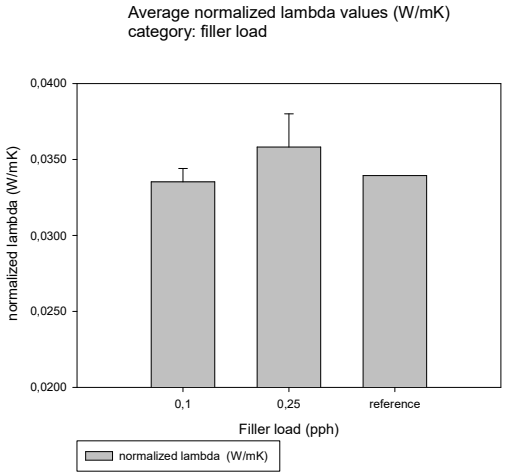


## 3.4 Modelling thermal conductivity of PU flexible foams with carbon nanotubes.

In mixing rule model, filler and matrix contribute independently to the overall thermal conductivity, in proportion to their relative volume fractions:

$$\lambda solid = (1-\delta)\lambda_{PU\,s} + \delta\,\lambda_{SWCNT} \quad (9)$$

Where δ is the volume fraction of filler; thermal conductivities of carbon nanotubes and pure PU polymeric matrix are $\lambda_{SWCNT}$ and $\lambda_{PU\,s}$ respectively.

It is well known that experimental conductivity values obtained from SWCNT – composites are normally far away from predicted values obtained by application of mixing rule [27] [28]. That is due to the effect of interfacial resistance between SWCNT´s filler edges and polymeric matrix. Because of that, optical phonons mainly responsible for heat transmission within carbon nanotubes are partially scattered through the host medium interface and energy available for heat transfer is lowered.

A model for prediction of thermal conductivity for randomly oriented ellipsoidal fillers in a host medium was developed by Kapitza [29] and adapted for composite materials by Nan and Berringer [30] [13]. Thermal conductivity of solid phase according this model is depending of interfacial resistance $R_k$ ($m^2K/W$) as follows:

$$\lambda solid = \lambda_{PU\,s} \frac{(3+\delta(\beta\perp+\beta\parallel)}{(3-\delta\beta\perp)} \qquad (10)$$

Where

$$\beta\perp = \frac{2(d(\lambda_{SWCNT}-\lambda_{PU\,s})-2R_K\lambda_{SWCNT}\lambda_{PU\,s}}{d(\lambda_{SWCNT}+\lambda_{PU\,s})+2R_K\lambda_{SWCNT}\lambda_{PU\,s}} \qquad (11)$$

$$\beta\parallel = \frac{L(\lambda_{SWCNT}-\lambda_{PU\,s})-2R_K\lambda_{SWCNT}\lambda_{PU\,s}}{L\lambda_{PU\,s}+2R_K\lambda_{SWCNT}\lambda_{PU\,s}} \qquad (12)$$

Average value of 5.000 W/ m K has been considered for $\lambda_{SWCNT}$ [2]. Volume fraction, diameter and length of carbon nanotubes are "δ", "d" (considered value is 1,50 nm) and "L" (considered value is 1,7 μm ) respectively. It is also important to emphasize that Kapitza model estimates a value for solid phase conductivity under full percolating conditions.

Calculations of $\lambda solid$ by Kapitza model have been made for our PU-SWCNT system. Considered $R_k$ value for PU host medium is 2,49 E-09$m^2$ K/ W taken from [16]; δ values are obtained from mixing rates specified in table nr. 3.

As it can be seen in fig.11, Kapitza model provides values of $\lambda solid$ of the same order magnitude of real average values, specially for strategies 1 to 3. It is easily perceived that strategies 1 and 2 are not reaching Kapitza full percolation condition, which it is the case for strategy 3 and 4. Strategy 4 presents conductivity values that exceed significatively predicted values by Kapitza model, but still bellow mixing rule values: interfacial resistance used as a background doesn´t fit as well as it does in previous strategies; however this value provides a good approach to compare effectiveness of a single strategy with each other. We can now look for an explanation of results showed in fig.11 by introducing the concept of interfacial thickness, "h" defined as :

$$h = \frac{\lambda soli}{\Lambda} \qquad (13)$$

Where Λ is the interfacial thermal conductivity, and has units of W/$m^2$ K.

$$\Lambda = \frac{1}{Rk} \qquad (14)$$

For the planar interface geometry, "h" is equal to the matrix thickness over which the temperature drop is the same as at the interface [31]. Looking at fig.11 it seems clear that a high population of nanofillers did reach threshold interparticle distance in strategy nr. 3. In the case of strategy 4 this interparticle distance has been even reduced because a higher performance of this dispersion technique", therefore it will be difficult to improve even more this result (threshold value for interfacial distance is set in the order of 1 Å by introducing $\lambda solid$ and $R_k$ considered values in equation (13)). In the case of strategies with a lower performance (nrs. 1 and 2), only a low rate of particles did arrive to this threshold value.

In this section, the importance of $R_k$ has been confirmed as a limiting value for achieving higher conductivity values. It is necessary to emphasize the importance of the ratio between cell size and "L" (size factor). The highest the length of SWCNT is, the less the contribution of $R_k$ in the final thermal conductivity is detected, as less "interfacial steps" are along the system.

**Fig.11** *Comparison real obtained conductivity values vs. mixing rule and Kapitza model per process strategy (right).*

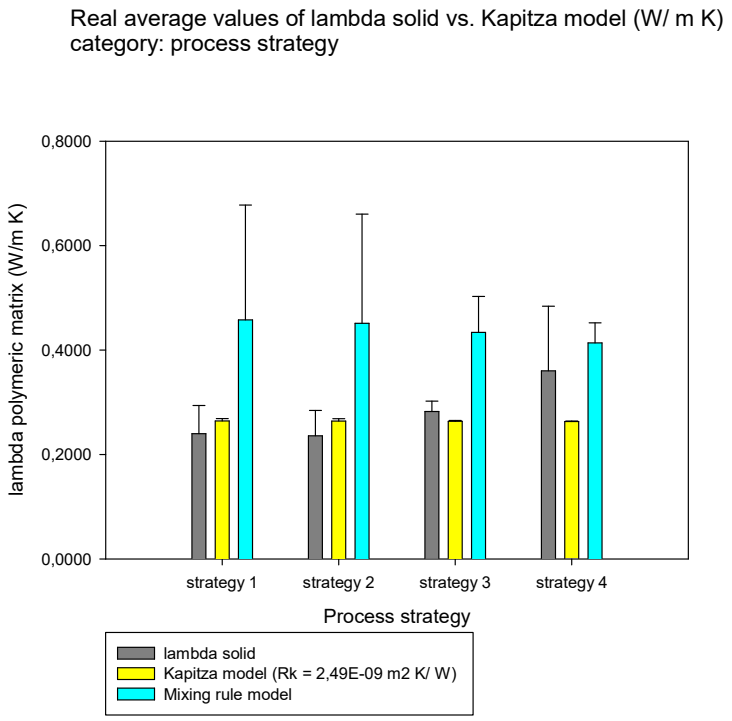


# 4.-Conclusions

Four strategies for deploying a full SWCNT percolating network inside flexible PU foams have been analysed. Level of percolation has been indirectly tracked by measuring thermal conductivity of samples by TPS method. To assess which is the most suitable strategy, solid phase conductivity for each produced part was evaluated by removing radiative (theoretically estimated using Rosseland & Glicksmann model), convective (assumed to be 0) and gas conductivity terms from total obtained conductivity values. It is well known that density and anisotropy ratio have a direct contribution to thermal conductivity. To ensure which is the real contribution of SWCNT apart from other indirect factors, a correction of density and anisotropy was made on solid phase conductivity to refer all samples to the same structural standard values (normalized conductivity values).

It has been proved consistently that "in situ" strategy nr.4 is the most suitable because interfacial distance between carbon nanotubes reach its minimum value, so that thermal conductivity for polymer matrix arrives at the maximum level Maximum conductivity gain vs. reference foam (pure) which is directly caused by SWCNT is 25,6%. Trials with longer SWCNT size ratios are suitable for improving this ratio.

It has also been observed a relationship between filler percolation and cellular structure. High percolation levels are followed by a change of morphology in cellular structure; big voids have also been observed in percolated samples, which size largely exceeds average cell estimated values in a first approach. This change is worth to be investigated in next research jobs. In a first approach, we suggest a resistance provided by the percolating network itself to its change from a high entropy level (fillers randomly distributed within dispersive solvent, stabilized by Van der Waal bondings) to a semi organized cellular structure.

Calculated solid conductivity values have been compared with values obtained from Kapitza and mixing rule models. $R_k$ value obtained from source [16] provides a background to compare effectiveness between different dispersion techniques. Direct thermal conductivity measurement of samples using stationary method, also the obtention of radiative and terms from experimental sources are also suitable to improve accuracy, but not confidence on final results.

## Acknowledgments

I would like to acknowledge the support of Cellmat laboratory team during experimental phase of this research, also the valuable contributions of Ester Laguna and Miguel Ángel Rodríguez-Pérez during the preparation of this manuscript.

## References

[1] J. Hone, M. Whitney, C. Piskoti, A. Zettl, «Thermal conductivity of single-walled carbon nanotubes,» *Physical review B,* vol. 59, nº 4, pp. 2514-2516, 1999.

[2] C. Yu, L. Shi, Z. Yao,D. Li, A. Majumdar, «Thermal Conductance and Thermopower of an Individual Single-Wall Carbon Nanotube,» *Nano Letters,* vol. 5, nº 9, pp. 1842-1846, 2005.

[3] P. Kim, L. Shi, A. Majumdar, P. L. McEuen, «Thermal Transport Measurements of Individual Multiwalled Nanotubes,» *Physical Review Letters,* vol. 87, nº 21, pp. 215502-1; 215502-4, 2001.

[4] J. Hone, M.C. Llaguno, M.J. Biercuk, A.T. Johnson, B. Batlogg, Z. Benes, J.E. Fischer, «Thermal properties of carbon nanotubes and nanotube-based materials,» *Appl. Phys. A,* vol. 74, pp. 339-343, 2002.

[5] Y. Xu, G. Ray, B. Abdel-Magid, «Thermal behavior of single-walled carbon nanotube polymer–matrix composites,» *Composites: Part A,* vol. 37, pp. 114-121, 2006.

[6] J.Hong, J.Lee, C.K Hong, S.E Shim, «Effect of dispersion state of carbon nanotube on thermal conductivity of poly(dimethyl siloxane) composites,» *Current Applied Physics,* vol. 10, pp. 359-363, 2010.

[7] W.Hong, N.Tai, «Investigations on the thermal conductivity of composites reinforced with carbon nanotubes,» *Diamond & Related Materias,* vol. 17, pp. 1577-1581, 2008.

[8] S. Ghose, K.A. Watson, D.C. Working, J.W. Connell, J.G. Smith Jr., Y.P. Sun, «Thermal conductivity of ethylene vinyl acetate copolymer/nanofiller blends,» *Composites Science and Technology,* vol. 68, pp. 1843-1853, 2008.

[9] J. A. King, D. L Gaxiola, B. A. Johnson & J.M Keith, «Thermal Conductivity of Carbon-filled Polypropylene-based Resins,» *Journal of Composite Materials,* vol. 44, nº 7, pp. 839-855, 2010.

[10] H. Xia, M. Song, «Preparation and characterization of polyurethane–carbon nanotube composites,» *Soft Matter,* vol. 1, pp. 386 - 394, 2005.

[11] R. Verdejo, R. Stämpfli, M. Alvarez-Lainez, S. Mourad, M.A. Rodriguez-Perez, P.A. Brühwiler,M. Shaffer, «Enhanced acoustic damping in flexible polyurethane foams filled with carbon nanotubes,» *Composites Science and Technology,* vol. 69, pp. 1564-1569, 2009.

[12] Jenny Hilding, Eric A. Grulke, Z. George Zhang, F. Lockwood, «Dispersion of Carbon Nanotubes in Liquids,» *Journal of Dispersion Science and Technology,* vol. 24, nº 1, pp. 1-41, 2003.

[13] Ce-Wen Nan, R.Birringer, D.R Clarke, H.Gleiter, «Effective thermal conductivity of particulate composites with interfacial thermal resistance,» *Journal of Applied Physics,* vol. 81, nº 10, pp. 6692-6699, 1997.

[14] H. Yoon, M. Yamashita, S. Ata, D. N. Futaba, T. Yamada, K. Hata, «Controlling exfoliation in order to minimize damage during dispersion of long SWCNTs for advanced composites,» *Scientific Reports,* vol. 4, nº 3907, pp. 1-8, 2014.

[15] P.C Maa, N. A. Siddiqui, G. Marom, J.K Kim, «Dispersion and functionalization of carbon nanotubes for polymer-based nanocomposites: A review,» *Composites: Part A,* vol. 41, pp. 1345-1367, 2010.

[16] M.B Brying, D.E Milkie, M.F Islam, J.M Kikkawa, G.Yodh, «Thermal conductivity and interfacial resistance in single-wall carbon epoxy composites,» *Applied Physics Letters,* vol. 87, p. 161909, 2005.

[17] L. R. Glicksman, «Heat transfer in foams (chap.5),» de *Low density cellular plastics, physical basis of behaviour.*, 2 ed., Springer -Science business media, B.V, 1994.

[18] M. Alvarez Lainez, M. A. Rodriguez-Pérez, J. A. De Saja, «Thermal Conductivity of Open-Cell Polyolefin Foams,» *Journal of Polymer Science: Part B: Polymer Physics,* vol. Vol. 46, pp. 212-221, 2008.

[19] S. Pardo-Alonso, E. Solórzano , S. Estravís , M. A. Rodríguez-Perez, J. A. de Saja, «In situ evidence of the nanoparticle nucleating effect in polyurethane–nanoclay foamed systems,» *Soft Matter,* vol. 8, nº 44, p. 11262-11270, 2012.

[20] S. Estravís, J. Tirado-Mediavilla, M. Santiago-Calvo, J. L. Ruiz-Herrero, F. Villafañe, M. A. Rodríguez-Pérez, «Rigid polyurethane foams with infused nanoclays: Relationship between cellular structure and thermal conductivity,» *European Polymer Journal,* vol. 80, pp. 1-15, 2016.

[21] Y. A. Çengel y A. J. Ghajar, «Transferencia de calor y masa. Fundamentos y aplicaciones,» 3ª ed., Mc Graw Hill, 2007.

[22] J. Holman, de *Heat Transfer*, McGraw-Hill, 2010.

[23] Ashby, M.F, Materials Selection in Mechanical Design; 3rd Edition, Butterworth-Heinemann, 2005.

[24] O. Almanza, M. A. Rodriguez Pérez, J. A. De Saja, «Applicability of the Transient Plane Source Method To Measure the Thermal Conductivity of Low-Density Polyethylene Foams,» *Polymer Physics,* vol. 42, pp. 1226-1234, 2004.

[25] Pinto J., Solórzano E., Rodriguez-Perez MA., de Saja JA., «Characterization of the cellular structure based on user-interactive image analysis procedures,» *Journal of Cellular Plastics,* vol. 49, nº 6, pp. 555-575, 2013.

[26] L. Glicksman, «Heat transfer and ageing of cellular foam insulation,» *Cellular Polymers,* vol. 10, pp. 276-293, 1991.

[27] Scott T. Huxtable, D. G. Cahill, S. Shenogin, L. Xue, R. Ozisik,, «Interfacial heat flow in carbon nanotube suspensions,» *Nature materials,* vol. 2, pp. 731-734, Nov. 2003.

[28] H. Chen, V. V. Ginzburgb, J. Yang, Y. Yanga, W. Liua, Y. Huanga, L. Dua, B. Chen, «Thermal conductivity of polymer-based composites: Fundamentals and applications,» *Progress in Polymer Science,* vol. 59, pp. 41-85, 2016.

[29] P. Kapitza, *J.Phys. (Moscow),* vol. 4, n° 181, 1941.

[30] Ce-Wen Nan, G.Liu, Y.Liu, M.Li, «Interface effect on thermal conductivity of carbon nanotube composites,» *Applyed Physics Letters,* vol. 85, n° 16, pp. 3549-3551, 2014.

[31] S. Shenogin, L. Xue, R. Ozisik, P. Keblinski, D. G. Cahill, «Role of thermal boundary resistance on the heat flow in carbon-nanotube composites,» *Journal of Applied Physics,* vol. 95, n° 12, pp. 8136-8144, 2004.

[32] F. H. Gojny, M. H.G. Wichmann, B. Fiedler, I. A. Kinloch, W. Bauhofer, A. H. Windle, K. Schulte, «Evaluation and identification of electrical and thermal conduction mechanisms in carbon nanotube/epoxy composites,» *Polymer,* vol. 47, pp. 2036-2045, 2006.

[33] R.Taranum,M.Abbas,L.K Mishra, «An Evaluation of temperature Dependent Thermal Conductivity of Carbon Nanotube,» *J.Pure Appl. & Ind. Phys,* vol. 3, n° 4, pp. 291-300, 2013.